SIMULATING THE 1755 TSUNAMI PROPAGATION IN PRESENT-DAY LISBON WITH A SHALLOW-WATER MODEL

SIMULAÇÃO DA PROPAGAÇÃO DO TSUNAMI DE 1755 NA ATUAL FRENTE RIBEIRINHA DE LISBOA COM EQUAÇÕES DO TIPO SAINT-VENANT

D. Conde
CEHIDRO /// Instituto Superior Técnico - UTL

R. Canelas
CEHIDRO /// Instituto Superior Técnico - UTL

J. Murillo
University of Zarazoza /// Fluid Mechanics C.P.S.

R.M.L. Ferreira
CEHIDRO /// Instituto Superior Técnico - UTL

ABSTRACT: A recent revision of the catalogue of tsunamis in Portugal has shown that Tagus estuary has been affected by catastrophic tsunamis numerous times over the past two millennia. This justifies the modelling efforts aimed at quantifying potential inundation areas for present-day altimetry and bathymetry of Tagus estuary. The purpose of this work is to present a 2DH mathematical model applicable to discontinuous shallow flows over complex geometries such as tsunami propagation overland. The conceptual model and the discretization scheme are presented and validation tests are described. The propagation of a tsunami with the magnitude of that of 1755 is simulated for the bathymetric and altimetry conditions of present day Tagus estuary. The study shows that some locations of Tagus estuary are vulnerable to tsunami impacts, as they may register 1 to 2m flow depths and velocities of 5ms^{-1}.

Keywords: mathematical modelling, tsunami, Tagus estuary.

RESUMO: Uma revisão recente do histórico de tsunamis em Portugal mostrou que o estuário do Tejo foi afetado por vários tsunamis catastróficos nos dois milénios mais recentes. Tal facto justifica os esforços de modelação com o objetivo de quantificar áreas de potencial inundação no estuário do Tejo, considerando as suas condições altimétricas e batimétricas atuais. O propósito deste trabalho é apresentar um modelo matemático 2DH aplicável a escoamentos descontínuos em águas pouco profundas com geometrias de fundo complexas, como é o caso da propagação em terra de um tsunami. Apresenta-se neste artigo o modelo conceptual e o esquema de discretização, bem como uma descrição dos testes de validação efetuados. Foi efetuada a simulação de um tsunami com a mesma magnitude do que destruiu Lisboa em 1755, considerando no entanto as condições de altimetria e batimetria do presente. Este estudo mostra que alguns locais do estuário do Tejo estão vulneráveis ao impacto de um tsunami de tal proporção, com alturas de escoamento de 1 a 2m e velocidades da ordem de 5m/s.

Palavras-chave: modelação matemática, tsunami, estuário do Tejo.

1. INTRODUCTION

Tsunamis are waveforms mostly originated by the vertical displacement of the seafloor as a consequence of an earthquake, by internal or external landslides (that can also be triggered by earthquakes), or by volcanic eruptions. They propagate in the ocean as long waves carrying a large amount of kinetic energy. In deep waters, they exhibit low amplitude, relatively to the mean local sea level, which makes them difficult to observe directly. As they travel up the continental slope, the wavelength typically reduces and the amplitude increases. The name tsunami, loosely translated as harbour waves, addresses this feature, the fact that the wave becomes visible only after shoaling. Approaching shore, the waves may break and form bores that propagate overland (Yeh, 1991). At this stage the tsunami becomes particularly destructive as its large amount of momentum is imparted to the obstacles it encounters. It incorporates debris, either natural sediment eroded from the bottom boundary or remains of human built environment, as seen in the recent 2004 and 2011 occurrences in Sumatra and Japan, respectively.

A recent revision of the catalogue of tsunamis in Portugal has shown that Tagus estuary has been affected by catastrophic tsunamis numerous times over the past two millennia (Baptista *et al.* 2009). This justifies the modelling efforts aimed at quantifying potential inundation areas for present-day altimetry and bathymetry of Tagus estuary. Such modelling efforts have been undertaken recently (Baptista *et al.* 2011) but improvements can be achieved both in conceptual model and discretization techniques.

The objectives of this work are: i) to present a 2DH mathematical model applicable to discontinuous flows over complex geometries such as tsunami propagation overland and ii) to apply the model to the propagation of a tsunami with the magnitude of that of 1755 in the Lisbon waterfront. The model is based on conservation equations of mass and momentum, derived within the shallow water hypothesis, constituting a quasi-linear hyperbolic system of conservation laws.

Particularly robust numerical discretization techniques within the finite-volume framework have been developed by Murillo & García-Navarro (2010) allowing for fully conservative solutions to initial value problems (IVPs). Also, advances have been achieved in discretization of the non-homogeneous terms related to bed slope leading to well-balanced schemes (Toro, 2001, Vázquez-Cendón, 1999). A robust wetting-drying algorithm, entropy conditions to prevent non-physical shocks and a revised Courant condition have also been proposed by Murillo & Garcia-Navarro (2010). These advances in numerical discretization have been introduced in the present simulation tool.

Finite-volume techniques are compatible with body-fitting unstructured meshes. This allows for optimization of computational effort, since the domain can be discretized with large cells, where flow gradients are small, and with small cells in the vicinity of flow obstacles (such as buildings) and, in general, where flow gradients are expected to be large. This requires good articulation of numerical discretization with GIS tools, an issue addressed with care in the present model.

The conceptual model, the fundamentals of the discretization approach, validation tests and the simulation of the 1755 tsunami in present-day Tagus estuary are shown in the following sections.

2. CONCEPTUAL MODEL

2.1. Conservation equations

Tsunamis are shallow flows, even in ocean waters, since their wavelength is several orders of magnitude larger than the flow depth and the entire water column is in motion. Overland, the tsunami is normally propagated as a bore, i.e. a discontinuous flow featuring a wave-front. The shallow-water hypotheses are thus acceptable, at least when the wave has reached the continental shelf. Depth-integrating the Navier-Stokes equations with the appropriate kinematic boundary conditions for the bottom and for the free surface one obtains the conservation equations of mass and momentum in two orthogonal directions in the horizontal plane:

$$\partial_t h + \partial_x (hu) + \partial_y (hv) = 0 \tag{1}$$

$$\partial_t (uh) + \partial_x \left(u^2 h + \tfrac{1}{2} g h^2\right) + \partial_y (uvh) = - gh\partial_x Z_b - \frac{1}{\rho}\partial_x h T_{xx} - \frac{1}{\rho}\partial_y h T_{xy} - \frac{\tau_{b,x}}{\rho} \tag{2}$$

$$\partial_t (vh) + \partial_x (uvh) + \partial_y \left(v^2 h + \tfrac{1}{2} g h^2\right) = - gh\partial_y Z_b - \frac{1}{\rho}\partial_y h T_{yy} - \frac{1}{\rho}\partial_x h T_{yx} - \frac{\tau_{b,y}}{\rho} \tag{3}$$

O texto deste artigo foi submetido para revisão e possível publicação em outubro de 2012, tendo sido aceite pela Comissão de Editores Científicos Associados em outubro de 2012. Este artigo é parte integrante da ***Revista Recursos Hídricos***, Vol. 33, Nº 2, 25-35, novembro de 2012.
 ISSN 0870-1741 | DOI 10.5894/rh33n2-2

where x, y are the space coordinates, t is the time coordinate, h is the flow depth, u and v are the depth-averaged velocities in the x and y directions, respectively, Z_b is the bed elevation, ρ represent the water density (salt water for ocean borne tsunamis), T_{ij} (i or j=1 stands for x and i or j=2 stands for y) are the depth-averaged turbulent stresses and τ_b is the bottom shear stress.

It is noted that system (1) to (3) does not include dispersive terms and the Coriolis term. Dispersive terms would be relevant in case of tsunamis generated by landslides (Antunes do Carmo, 2000; Liu *et al.* 2005) and less important when the tsunami is caused by sea floor upwelling. Dispersive terms are surely negligible in the run-up stage, i.e. when the tsunami propagates overland (Kanoglu & Synolakis, 1998). Since this paper is mostly concerned with this stage, no dispersive terms were included in the system of conservation laws. As for the Coriolis term, it may be relevant in deep waters, where the tsunami wavelength is high: for a typical wavelength of 100 km, a tsunami traveling in the Atlantic ocean between the Gorringe Ridge and Lisbon (where the mean depth is about 800 m) would have a Coriolis parameter $f_c = 27.3\text{x}10^{-5}\ \sin(36\pi\ /\ 180)=$ $=8.6\text{x}10^{-5}$ and a Rossby number ($\sqrt{9.8\times800}\ /\ \left(f_c 100\times10^3\right)$) of 10.3. Approaching shore, the wavelengths characterizing the tsunami are much smaller, approximately an order of magnitude smaller. In this case, the Rossby number is approximately 25.2, high enough to render Coriolis effects negligible. Since the present simulation is concerned with the propagation of the tsunami in the estuary of River Tagus, the Coriolis term is neglected. The effect of Coriolis force, however, is present in the waves that are introduced in the oceanic boundary condition, calculated by Baptista *et al.* (2011).

Conservation laws (1) to (3) form a quasi-linear hyperbolic system of partial differential equations. Hyperbolicity implies that all wave-forms will eventually break (Whitham, 1974) and form the discontinuous wave-front or bore that characterizes tsunami propagation overland. The energy dissipated in the breaking process is not accounted for in the model. However, the more relevant energy loss associated to the propagation of the bore is included in the model by virtue of Rankine-Hugonoit shock conditions, captured by the numerical scheme.

2.2. Closure equations

The bed shear stress, τ_b, is such that

$$|\tau_{\mathbf{b}}| = \rho C_f\, |\mathbf{u}|^2 \tag{4}$$

The friction coefficient, C_f, can be expressed by the Manning-Strickler formula ($C_f = g\,/(h^{1/3}\,K^2)$ where K is Strickler's coefficient whose dimensions are $\text{L}^{1/3}\,\text{T}^{-1}$) or, if the wave carries debris, by the formula proposed by Ferreira *et al.* (2009), $C_f = \text{u}d_s\,/\,(h\,\omega_s)$, where d_s and ω_s are the sediment diameter and settling velocity, respectively. The turbulent stress tensor is given by,

$$T_{ij} = \rho \nu_T \left(\partial_{x_j} u_i + \partial_{x_i} u_j\right) \tag{5}$$

where the eddy viscosity, ν_T, is expressed by the following simplified zero-equation K -ϵ model (Pope, 2000),

$$\nu^T = C_\mu \frac{\kappa^2}{\epsilon} \tag{6}$$

where C_μ=0.09 (Pope, 2000, p. 374), K is the depth-averaged turbulent kinetic energy (TKE) and ϵ is the depth-averaged rate of TKE dissipation. Using the experimental data of Ferreira (2005),

$$\kappa = 4.375 u_*^2 \quad \text{and} \quad \epsilon = 5\frac{u_*^3}{h} \tag{7}$$

where u_* is the friction velocity given by,

$$u_* = \sqrt{|\tau_b|/\rho} \tag{8}$$

3. DISCRETIZATION TECHNIQUE

The hyperbolic, non-homogeneous, first order, quasi-linear system of conservation laws, equations (1) to (3), can be written in compact notation:

$$\partial_t \mathbf{U}(\mathbf{V}) + \partial_x \mathbf{F}(\mathbf{U}) + \partial_y \mathbf{G}(\mathbf{U}) = \mathbf{H}(\mathbf{U}) \tag{9}$$

with,

$$\mathbf{V} = \begin{bmatrix} h \\ u \\ v \end{bmatrix};\quad \mathbf{U} = \begin{bmatrix} h \\ uh \\ vh \end{bmatrix};\quad \mathbf{F} = \begin{bmatrix} uh \\ u^2 h + \frac{1}{2} g h^2 \\ uvh \end{bmatrix};$$

$$\mathbf{G} = \begin{bmatrix} vh \\ vuh \\ v^2 h + \frac{1}{2} g h^2 \end{bmatrix} \quad \text{and} \quad \mathbf{H} = \begin{bmatrix} 0 \\ -gh\partial_x Z_b - \tau_x/\rho \\ -gh\partial_y Z_b - \tau_y/\rho \end{bmatrix},$$

where V and U are the vectors of primitive and conservative dependant variables, respectively, F and G are the flux vectors, in x and y direction, H is the vector of source terms and $\tau_i = \tau_{b,i} + \partial_{x_i} hT_{ii} + \partial_{x_j} hT_{ij}$. Employing Godunov's finite-volume approach (Leveque, 2002), discretization, the system (9) is integrated in a cell i. The following explicit flux-based finite-volume scheme is obtained,

$$\mathbf{U}_i^{n+1} = \mathbf{U}_i^n - \frac{\Delta t}{A_i}\sum_{k=1}^{3} L_k \sum_{m=1}^{3}\left(\tilde{\lambda}^{(m)}\alpha^{(m)} - \beta^{(m)}\right)_{ik}^{-}\tilde{\mathbf{e}}_{ik}^{(m)} + \Delta t\left(\mathbf{R}_i^{n+1}\right) \quad (10)$$

where Δt is the time step, obeying a Courant condition ($CFL \leq 1$), A_i is the cell area, L_k is the edge length, and $\tilde{\lambda}^{(m)}$ and are the m-th approximate eigenvectors and eigenvalues, respectively, defined as (Roe, 1981)

$$\tilde{\lambda}_{ik}^{(1,3)} = \left(\tilde{u}\cdot n \pm \tilde{c}\right); \quad \tilde{\lambda}_{ik}^{(2)} = \left(\tilde{u}\cdot n\right) \quad (11)$$

$$\begin{aligned}
\tilde{e}_{ik}^{(1)} &= \begin{bmatrix} 1 & \tilde{u} - \tilde{c}\cdot n_x & \tilde{v} - \tilde{c}\cdot n_y \end{bmatrix}_{ik}^{T} \\
\tilde{e}_{ik}^{(2)} &= \begin{bmatrix} 0 & -\tilde{c}\cdot n_y & \tilde{c}\cdot n_x \end{bmatrix}_{ik}^{T} \\
\tilde{e}_{ik}^{(3)} &= \begin{bmatrix} 1 & \tilde{u} + \tilde{c}\cdot n_x & \tilde{v} + \tilde{c}\cdot n_y \end{bmatrix}_{ik}^{T}
\end{aligned} \quad (12)$$

with,

$$\tilde{u}_{ik} = \frac{u_i\sqrt{h_i} + u_j\sqrt{h_j}}{\sqrt{h_i} + \sqrt{h_j}}; \quad \tilde{v}_{ik} = \frac{v_i\sqrt{h_i} + v_j\sqrt{h_j}}{\sqrt{h_i} + \sqrt{h_j}}; \quad \tilde{c}_{ik} = \sqrt{g\frac{h_i + h_j}{2}} \quad (13)$$

where $\tilde{u}$ and $\tilde{v}$ denote the x and y direction approximate velocities and $\tilde{c}$ is the approximate free-surface disturbances celerity.

The wave strengths associated to conservative and non-conservative ($gh\partial_{xi} Z_b$) fluxes are denoted by $\alpha^{(m)}$ and $\beta^{(m)}$, respectively, and are given by,

$$\begin{aligned}
\alpha_{ik}^{(1)} &= \frac{\Delta_{ik}(h)}{2} - \frac{1}{2\tilde{c}_{ik}}\left(\Delta_{ik}\langle uh\rangle - \tilde{u}_{ik}\Delta_{ik}\langle h\rangle\right)\cdot n_{ik} \\
\alpha_{ik}^{(2)} &= \frac{1}{\tilde{c}_{ik}}\left(\Delta_{ik}\langle uh\rangle - \tilde{u}_{ik}\Delta_{ik}\langle h\rangle\right)\cdot t_{ik} \\
\alpha_{ik}^{(3)} &= \frac{\Delta_{ik}(h)}{2} - \frac{1}{2\tilde{c}_{ik}}\left(\Delta_{ik}\langle uh\rangle - \tilde{u}_{ik}\Delta_{ik}\langle h\rangle\right)\cdot n_{ik}
\end{aligned} \quad (14)$$

$$\beta_{ik}^{(1)} = -\frac{1}{2\tilde{c}_{ik}}\left(\frac{p_b}{\rho^{(w)}}\right); \quad \beta_{ik}^{(2)} = 0; \quad \beta_{ik}^{(3)} = -\beta_{ik}^{(1)} \quad (15)$$

and R the parcel of the source terms not susceptible to be treated as a non-conservative fluxes.

$$\mathbf{R}_i^{n+1} = \left(\begin{bmatrix} \partial_t Z_b & -\tau_x / \rho_m & -\tau_y / \rho_m \end{bmatrix}^T\right)_i^{n+1} \quad (16)$$

Terms with $gh\partial_{xi} Z_b$ are not physical fluxes; they are treated as so to obtain a well-balanced numerical scheme (Vásquez-Cendón, 1999). Only the negative part of the eigenvalues $\tilde{\lambda}_{ik}^{(m)}$ and of $\beta_{ik}^{(m)}$ coefficients are used, ensuring that only incoming fluxes are used in the update of the conserved variables. The approximate eigenvalues and eigenvectors and the wave strengths are calculated as in Murillo *et al.* (2010).

The shear-rate in the definition of the depth averaged turbulent stresses, equation (5), is calculated from directional derivatives. The discretized directional derivative $\nabla_{ab} F$, of a generic differentiable variable F in the direction of the vector r_{ba} that connects the barycentres of cells $\boldsymbol{a}$ and $\boldsymbol{b}$ is,

$$D_{ab} = \frac{F(x_b, y_b) - F(x_a, y_a)}{\mathbf{r}_{ab}} \quad (17)$$

At each triangular cell, three directional derivatives can be defined, for each of the neighbouring cells. In a Cartesian referential the directional derivatives are written as $\nabla_{ab} F = \nabla F.\mathrm{e}_{r\,ab}$, where $\mathrm{e}_{r\,ab}$ is the directional unit vector and $\nabla = \partial_x + \partial_y$. With the unknowns as the gradients in the Cartesian referential, a pair of directional derivatives can be used to calculate $\partial_x F$ and $\partial_y F$. In general,

$$\begin{pmatrix} D_{ab} \\ D_{ac} \end{pmatrix} = \begin{pmatrix} \cos(\eta_{ab}) & \sin(\eta_{ab}) \\ \cos(\eta_{ac}) & \sin(\eta_{ac}) \end{pmatrix}\begin{pmatrix} \partial_x F \\ \partial_y F \end{pmatrix} \quad (18)$$

where η_{ab} and η_{ac} are the angles that the segments linking the barycentres of cells a and b and c, respectively, make with the x direction.

When cell-averaging the solution, the time step is chosen small enough to guarantee that there is no interaction between waves obtained as the solution of the Riemann Problem (RP) at adjacent cells. The stability region considering the homogeneous part of the system becomes,

$$\Delta t \le CFL\ \Delta t^{\tilde{\lambda}}; \qquad \Delta t^{\tilde{\lambda}} = \frac{\min(\chi_i, \chi_j)}{\max|\tilde{\lambda}^{(m)}|_{m=1,2,3}} \tag{19}$$

where the CFL value is less than one and,

$$\chi_i = \frac{A_i}{\max(L_k)_{i,k=1,2,3}} \tag{20}$$

In wet/dry interfaces with discontinuous bed level, the time step can become practically zero since negative fluid depths can be expected and enforcing positivity requires a very small time step. In order to ensure positivity for all cases and, at the same time, keeping the computational time step at acceptable levels, the fluxes for the update of the conserved variables obey (Murillo & García-Navarro, 2010)

$$\begin{aligned}
&\text{If } h_j^n = 0 \text{ and } h_j^{***} < 0 \text{ then}\\
&\Delta(E-R)_{ik}^- = \Delta(E-R)_k \text{ and } \Delta(E-R)_{jk}^- = 0\\
&\text{If } h_j^n = 0 \text{ and } h_i^* < 0 \text{ then}\\
&\Delta(E-R)_{jk}^- = \Delta(E-R)_k \text{ and } \Delta(E-R)_{ik}^- = 0
\end{aligned} \tag{21}$$

These restrictions efficiently prevent the appearance of negative fluid depths: the flux is zero at cells where an intermediate step predicts negative flow depths. In areas were h approaches zero, the computation of the primitive variables $u=uh/h$ leads to potentially large round-off errors.
Instead of defining a threshold for h above which the cell is allowed momentum, a threshold for the flow depth (h_{min}) is set to compute velocities.
The strategy for entropy correction, to avoid the possible non-physical solutions generated by Roe's approximate Jacobian, is drawn from the work by Murillo & García-Navarro (2010), were the objective is to forcefully promote the propagation of information in any occurring expansion wave by diffusing any non-physical shock.

4. VALIDATION WITH THEORETICAL SOLUTIONS

The dam-break problem over fixed flat smooth beds is an IVP that admits theoretical solutions (Stoker, 1957). The fundamental non-dimensional parameters that describe the initial conditions are,

$$\begin{aligned}
\alpha &\equiv \left(h_R + \left|\min(0, Z_{b_l})\right|\right) \Big/ \left(h_L + \max(0, Z_{b_l})\right)\\
\delta &\equiv Z_{b_l} \Big/ \left(h_L + \max(0, z_{b_l})\right)
\end{aligned} \tag{22}$$

where h_R and h_L are the initial fluid depths of the right and left states, respectively, and Z_{b_l} is the bed elevation on the left side considering the right side as the reference horizontal plane (Ferreira, 2005). The solution, according to Lax theorem (Leveque, 2002), features two waves (shocks or rarefaction waves), separated by a constant state. When h_L=10.0m, h_R=1m, α=0.2 and δ=-0.1, the solution features a downstream-progressing shock, an upstream-progressing rarefaction wave and a discontinuity at the bed jump (Alcrudo & Benkhaldoum, 2001). The problem is 1D but the discretization is 2DH with triangular cells with an average side of 0.65 m for a channel 10.0 m wide. The numerical results, obtained with CFL = 0.8, are shown in Figure 1 (left), along with the theoretical solution.
The numerical solution reproduces correctly the analytical weak solution. The energy dissipation induced by the bottom source terms is correctly evaluated and the shock speeds are correctly described. The effects of the numerical dissipation are visible (as profile smoothing) in the interface between the left state and the expansion wave and between the constant intermediate states. When h_L=10.0m, α=0.1 and δ = -0.1, Figure 4.1 (right), the solution features a downstream-progressing expansion wave, an upstream-progressing rarefaction wave and a discontinuity at the bed jump. The computed solution correctly follows the structure of the theoretical solution. However, the velocity at the wave front is underestimated because of the flux reduction imposed by the wetting-drying algorithm.
The validation tests show that discontinuous solutions are correctly reproduced, although the effects of numerical diffusion, notably wave amplitude attenuation, are perceptible. Since the error associated to numerical diffusion is dependent on the size of the mesh elements, it is envisaged that the effect of diffusion becomes unnoticeable for very fine grids (at the expense of computational cost), becoming relevant only for coarse grids such as that used in this validation example.

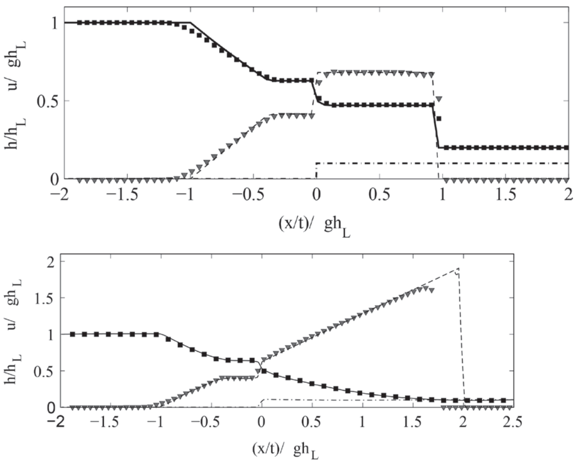

Figure 1 - Stoker solution with corresponding numerical solution. Left: $\alpha = 0.2$ and $\delta = -0.1$. Right: $h_L = 10.0$m, $h_R = 1$m, $\alpha = 0.1$ and $\delta = -0.1$.

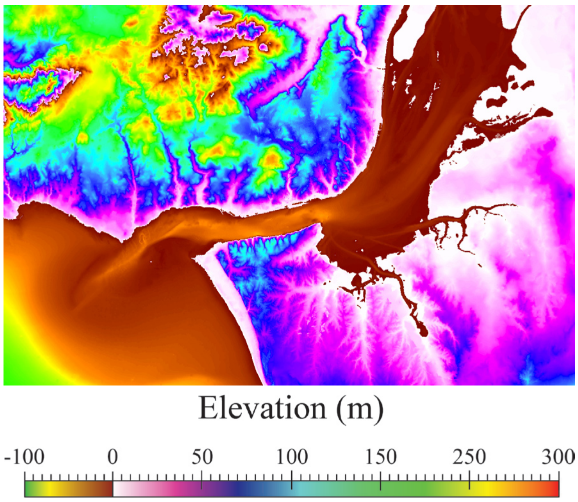

Figure 2 - Employed digital elevation model (10 m resolution).

5. APPLICATION: A 1755 TSUNAMI IN TODAY'S TAGUS ESTUARY

5.1. Initial and boundary conditions and mesh issues

The proposed model was employed to simulate a tsunami similar to that occurred in the 1st of November of 1755, in present-day Tagus estuary. Two scenarios were considered: low and high tide, defined as -2m and +2m, respectively, relatively to the mean sea level (reference zero). The digital elevation model including Tagus bathymetry, Figure 2, with a 10 m resolution and 1 m precision, was obtained from Luís (2007).
Open boundary conditions, formalised in terms of Rankine-Hugoniot conditions (Conde, 2012), are prescribed at the Tagus valley and at the Atlantic reach (Figure 3). In the Tagus valley a constant discharge of 500 m^3s^{-1} (approximately the modular discharge) is introduced in the direction normal to the boundary. In the Atlantic boundary, it is introduced, at each cell in the boundary, a water elevation time series corresponding to the 1755 tsunami, as calculated by Baptista *et al.* (2011). The main feature of these series is that they prescribe a water height, above tide level, of about 5 m at Bugio, in accordance to historical reports (Baptista *et al.* 2009). Figure 3 shows the first tsunami wave propagating over high tide, immediately after hitting Bugio. Water elevation, at Tagus mouth is about 7 m above reference zero, i.e. 5 m above high tide level.
Initial conditions comprise flow depths and velocities compatible with the discharge, at Tagus valley, of 500 m^3s^{-1} and tide level at the Atlantic boundary. The computational domain is composed of 125000 triangular cells, the smallest of which have 20 m long edges, Figure 4. Simulation covers 2.7 hours after Bugio island is hit. The results are shown in Figures 5 to 7.

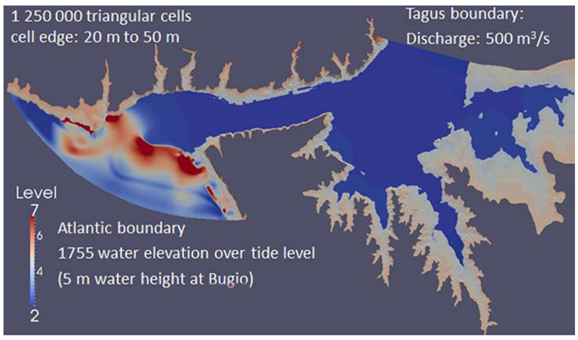

Figure 3 - Simulation at high tide. Initial and boundary conditions.

5.2. Results of the simulation

The main impacts of the tsunami propagating over a low tide level are shown in Figure 5, a detail of Lisbon Baixa. Inundation is limited to less than 1 m deep patches at Rocha do Conde de Óbidos, Cais do Sodré, Praça do Comércio and Sta. Apolónia. Velocities are

Figure 4 - Mesh topology examples at Lisbon waterfront: (Left) Belém and Alcântara (Right) downtown. (Red denotes inland cells and blue denotes riverbed cells).

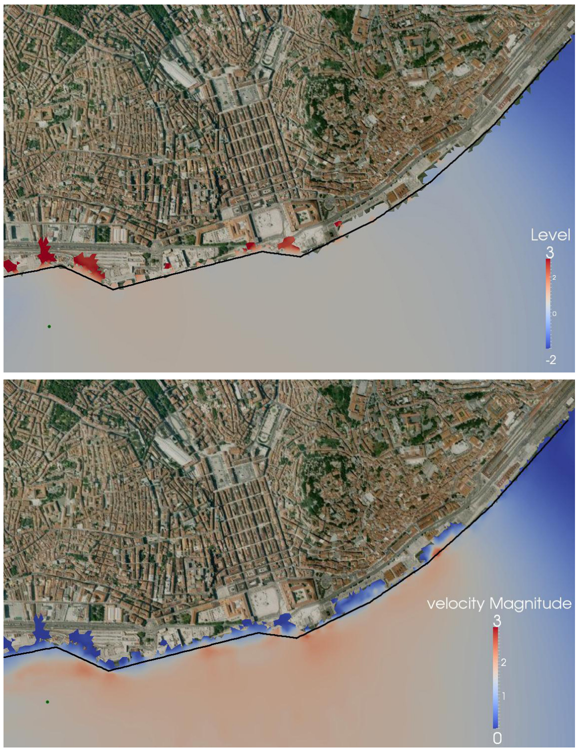

Figure 5 - Low tide simulation. Water elevation (left) and velocity (right) at Baixa waterfront 20 min after hitting Bugio.

low, less than 1 ms^{-1}. The extent of damage in this case would be limited, which is explained by the fact that landfills and protection works after 1755 left Lisbon waterfront about 5 m above low tide water elevation at the estuary if flow discharge at Tagus is low.

Figures 6 and 7 show the tsunami propagation on Lisbon waterfront at high tide. Figure 6 shows the results of the simulation at the Belém-Alcântara reach 9.5 to 14.5 min after the tsunami has hit Bugio. The simulation indicates that, in this case, the tsunami could have a devastating impact. The extent of penetration at Praça do Império and Jerónimos monastery could reach 500 m. At Alcântara, the largest penetration is about 550 m. Run-up (above local ground) can reach 2 m at Belém–Praça do Império and at Belém fortress. Flow velocities can reach 5 ms^{-1} at Alcântara harbour and at Belém.

Figure 7 shows the results of the simulation at high tide for the Baixa reach. Again, the simulation indicates that the tsunami would have major impacts on Lisbon waterfront. Praça do Comércio would be completely inundated and the wave would propagate inside Baixa network of orthogonal streets. Penetration would be about 300 m at Baixa and 400 m at S. Paulo. Water depths could reach 1.5 m at the shore line. Sta. Apolónia train station would also be reached by the incoming wave. Velocities of 3-4 ms^{-1} would be felt at Praça do Comércio at the beginning of the inundation and during draw-down.

The results of the simulation show larger inundation distances than those calculated by Baptista *et al.* (2006) and Baptista *et al.* (2011), which may be explained by the initial water elevation of the later study, coinciding with mean tide level and not high tide. Flow depths, however, are compatible with those calculated by Baptista *et al.* (2011) if the high tide level is added to the results of the latter study. Velocities are not susceptible to be compared as they are not calculated in Baptista *et al.* (2011).

The detailed patterns of flow are beyond the scope of the present simulation effort since the employed DEM does not have enough resolution to clearly distinguish streets and buildings. New simulations are under way in sensitive areas such as Belém, Alcântara and Baixa with actual street geometry.

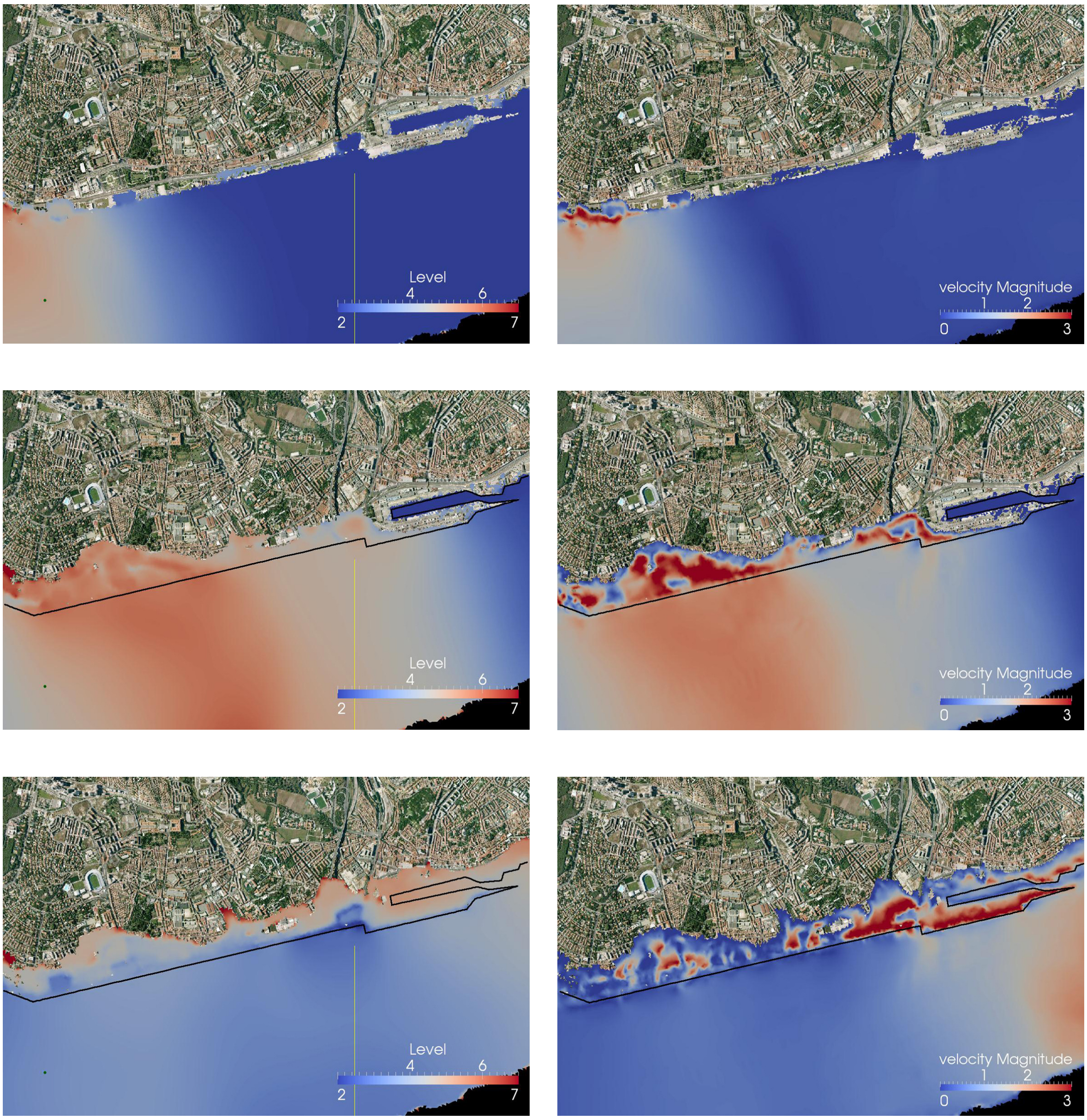

Figure 6 - High tide simulation. Water elevation (left) and velocity (right) at Belém-Alcântara waterfront 9.5, 11 and 14.5 min after hitting Bugio.

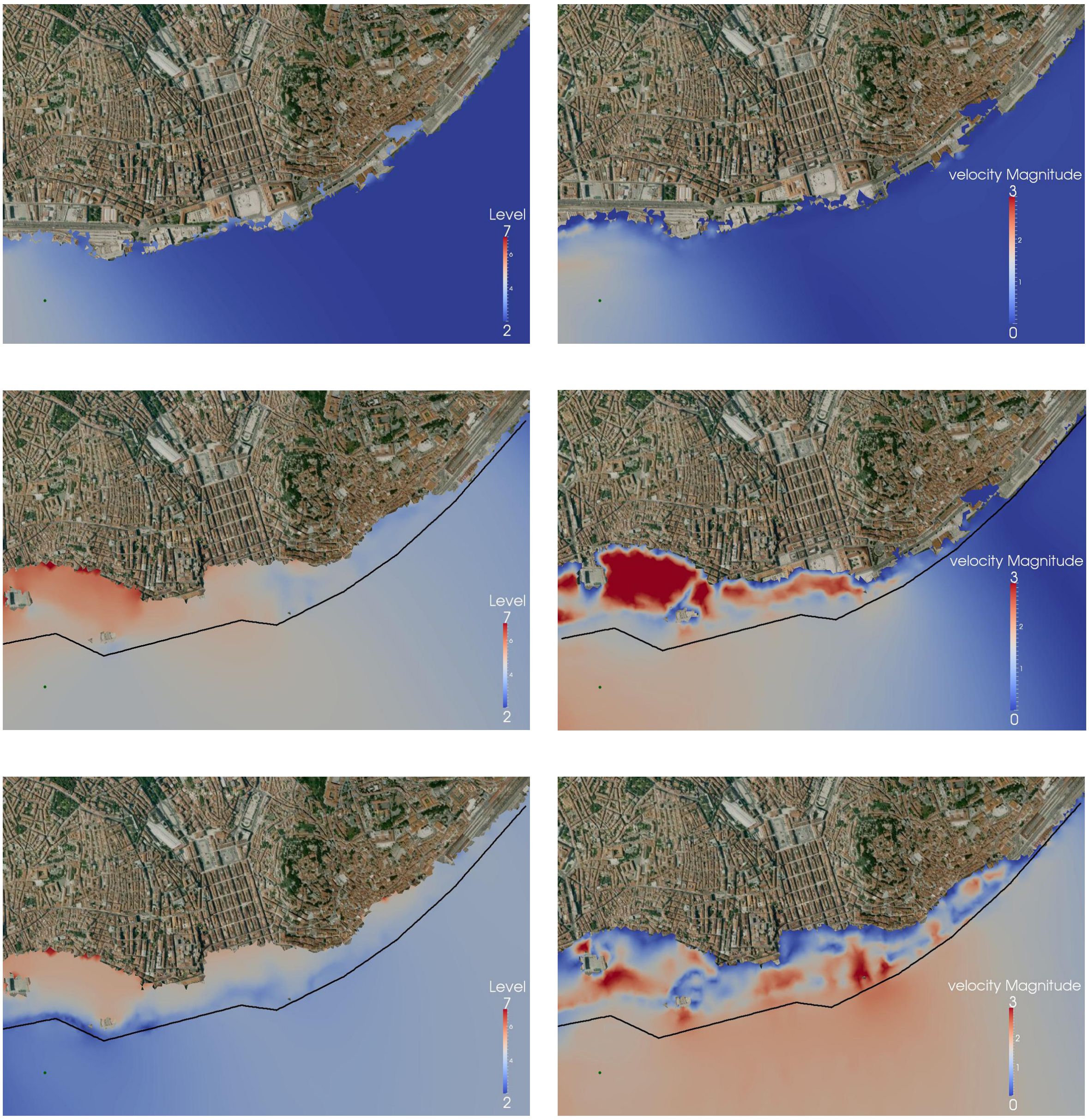

Figure 7 - High tide simulation. Water elevation (left) and velocity (right) at Baixa waterfront 15.5, 16.5 and 19.5 min after hitting Bugio.

6. CONCLUSION

The propagation of a tsunami with the magnitude of that of 1755 was simulated for the bathymetric and altimetry conditions of present day Tagus estuary. The simulated water elevations featured a maximum wave height of 5m above tide level at Bugio. The simulation tool was a mathematical model applicable to shallow flows that may develop bores or other type of discontinuities. The model has been validated with theoretical solutions.

At the Lisbon water front, the simulations show that the combination of high tide and tsunami can lead to major devastation in sensitive areas such as Belém, Alcântara, S. Paulo or Baixa. At these locations, the penetration of the inundation can reach 300 to 500 m. Flow depths may reach 1 to 2 m along the entire waterfront. The highest registered depths in the simulation occurred at Belém, in the vicinity of Belém fortress, an especially relevant touristic location. Velocities ranging between 4-5 ms^{-1} and 3-4 ms^{-1} would be felt at Praça do Comércio and Alcântara, both during run-up, and just slightly lower at draw-down. High velocities associated with above-waist flow depths are especially worrisome as they are responsible for incorporation of debris and are associated to high casualties.

The study has shown that some locations of Tagus estuary are vulnerable to tsunami impacts. More detailed studies, featuring actual building geometry, are under way. These should provide data to design evacuation plans in case of a major tsunami.

ACKNOWLEDGEMENT

Project "Exploração de imagens SAR para aperfeiçoar modelos de inundação no Rio Tejo (RIVERSAR-Exploiting SAR imagery to improve floodplain inundation models in the Tagus River)" (PTDC//CTE-GIX/099085/2008) has partially supported this research.

BIBLIOGRAPHY

Alcrudo, F. & Benkhaldoun, F. (2001). Exact solutions to the Riemann problem of the shallow water equations with a bottom step. *Computers and Fluids, 30*, 643–671.

Antunes do Carmo (2000). Tsunamis: geração e riscos. *Territorium, 7*: 15-24.

Baptista M.A.; Miranda, J.M.; Omira, R.; Antunes, C. (2011). Potential inundation of Lisbon downtown by a 1755-like tsunami. *Natural Hazards and Earth System Science*. 11, 3319-3326. doi:10.5194/nhess-11-3319-2011.

Baptista, M.A. & Miranda J.M. (2009). Revision of the Portuguese catalog of tsunamis. *Natural hazards and earth system sciences,* 9 (1): 25-42.

Baptista, M. A.; Soares, P. M.. ; Miranda, J. M. & Luis, J. F. (2006). Tsunami propagation along Tagus estuary (Lisbon, Portugal). Preliminary results, *Science of Tsunami Hazards,* 24(5), 329-328.

Conde, D. (2012). *A tsunami in Lisbon. Where to run?.* MSc dissertation, Instituto Superior Técnico, TU Lisbon.

Ferreira, R. M. L. (2005). *River Morphodynamics and Sediment Transport. Conceptual Model and Solutions*. Ph.D. thesis, Instituto Superior Técnico - Universidade Técnica de Lisboa, Lisboa.

Ferreira, R. M., Franca, M. J., Leal, J. G. & Cardoso, A. H. (2009). Mathematical modelling of shallow flows: Closure models drawn from grain-scale mechanics of sediment transport and flow hydrodynamics. *Canadian Journal of Civil Engineering,* 36, 1604–1621.

Kanoglu, U. & Synolakis, C.E. (1998). Long wave runup on piecewise linear topographies, *Journal of Fluid Mechanics,* 374, 1-28.

Leveque, R. (2002). *Finite Volume Methods for Hyperbolic Problems*. Cambridge University Press.

Liu, P. L.-F.; Wu, T.-R.; Raichlen, F.; Synolakis, C.E., & Borrero, J.C. (2005). Runup and rundown generated by three-dimensional sliding masses. *J. Fluid Mech.*, vol. 536, pp. 107–144.

Luis, J.F. (2007). Mirone: A multi-purpose tool for exploring grid data. *Computers & Geosciences,* 33, 31-41.

Murillo, J. & Garcia-Navarro, P. (2010). Weak solutions for partial differential equations with source terms: application to the shallow water equations. *J. Comp. Physics* 229(11), 4327–4368.

Murillo, J.; García-Navarro, P., Brufau, P. & Burguete, J. (2010). 2d modelling of erosion/deposition processes with suspended load using. *Journal of Hydraulic Research,* 46(1), 99–112.

Pope, S. B. (2000). *Turbulent Flows*. Cambridge University Press.

Roe, P. (1981). Approximate Riemann solvers, parameter vectors and difference schemes. *J. Comp. Physics* 43, 357–372.

Stoker, J.J. (1957). *Water waves. The mathematical with applications*. Willey Classic Library, (reprint of 1957 edition).

Toro, E. (2001). *Shock-Capturing Methods for Free Surface Shallow Flows.* Wiley, New York.

Vázquez-Cendón, M. (1999). Improved treatment of source terms in upwind schemes for the shallow water equations with irregular geometry. *J. Comp. Physics,* 148,497.

Viana-Baptista, M.A.; Miranda, J.M.; Omira, R.; Antunes, C. (2011). Potential inundation of Lisbon downtown by a 1755-like tsunami. *Natural Hazards and Earth System Science*. 11, 3319-3326. doi:10.5194/nhess-11-3319-2011.

Whitham, G. B. (1974). Linear and Non-Linear Waves. John Willey and Sons, Willey-Interscience. ISBN 0-471-94090-9.

Yeh, H.H. (1991). Tsunami bore runup. *Natural Hazards* 4(2-3), 209–220. DOI: 10.1007/BF00162788.